2005 American Control Conference
June 8-10, 2005. Portland, OR, USA

A Kalman Estimator for Detecting Repetitive Disturbances

Liang Chen[ab]
[a]Electrical Engineering Department
University of Shanghai for Science and Technology,
Jungong Lu 516, Shanghai 200093 China.
[b]Institut für Automatisierung und Informatik
Schlachthofstr. 4, 38855 Wernigerode, Germany
Tel. +49-(0)3943-6259746 Fax. +49-(0)3943-6259747.
lorenz.chen@gmx.de

Paolo Mercorelli[bd], Steven Liu[c]
[d]University of Applied Sciences Wolfsburg
Robert-Koch-Platz 8-a., 38440 Wolfsburg, Germany
Tel. +49-(0)5361-831615 Fax. +49-(0)5361-831602.
p.mercorelli@fh-wolfsburg.de
[c]Technische Universität Kaiserslautern
Erwin-Schrödiger-Straße D-67663 Kaiserslautern,
Germany
Tel. +49 (0)631 205 4535 sliu@eit.uni-kl.de

keywords: estimator, two-stage Kalman filter, disturbance estimation, electromagnetic actuator.

Abstract— **The paper proposes a two-stage Kalman filter combining a robust and optimal algorithm for state and disturbance estimation. A practical case coming from automotive application is studied in detail to show the effectiveness of the proposed technique.**

I. INTRODUCTION AND MOTIVATION

Recent works as [5], [6], [7] and [10] mark progresses in theoretical studies of two-stage Kalman filters. Especially their robustness and ability to deal with unknown input signals are important properties for real applications since in many situations dynamic disturbances can also be modelled as additional unknown inputs, and a robust state estimation is always an attractive means for advanced control concepts.

Recently, variable engine valve control has attracted a lot of attention because of its ability to improve fuel economy, reduce NOx emissions and increase torque performance over a wider range than conventional spark-ignition engine. Besides pure mechanical and electro-hydraulic variable valve train options, electromechanical valve actuators have been reported in the past years [2] and [8]. The control of such actuators is usually a high-dynamic non-linear problem with strong changing unknown external disturbances, therefore a very challenging issue. The high dynamic is needed since the valve opening and closing, following a desired velocity trajectory, has to be performed within a few milliseconds, leading to acceleration values of around 2500 m/s^2. At the same time, strong and varying disturbances caused by the gas pressure in the combustion chamber acting against the valves can affect significantly the valve opening process and the achievable trajectory accuracy. Furthermore, soft-landing is also an important control issue which means that the valve closing must be performed with a seating velocity under the value of about 0.1 m/s. Recent investigations, for example as reported in [4] and [9], show special considerations of disturbance rejection in their control system, e.g. applying a repetitive learning control based position measurement. In real application, however, it is often desirable to implement the control without position sensor due the very restricted mounting space and expense. In this case an estimator could be the basis for a sensorless control. On the other hand, the soft-landing turns out to be a difficult job which requires a highly precise state estimation.

The organization of this paper is the following: section II is devoted to the physical system and mathematical model description. In section III a two-stage Kalman filter is developed for the state and disturbance estimation. Simulation results and some conclusion remarks close the paper.

II. GENERAL CONSIDERATIONS AND PHYSICAL SYSTEM

Fig. 1 shows the operation principle of the engine valves to be controlled. Valves make the engine to breath. The intake valve allows air and fuel rushing into the cylinder so combustion can take place. The exhaust valve releases the spent fuel and air mixture from the cylinder. It is obvious that the timing of the valve opening and closing essentially influences the engine efficiency and fuel economy. The optimal choice of the opening and closing timing depends on the simultaneous operation conditions of the engine and should therefore be controlled individually. In conventional spark-ignition engines the valves are driven by the camshaft and their timing is fixed to the engine speed. The use of electromagnetic valve actuators decouples the valve timing from the engine speed and ensures the fully timing variability.

Fig. 2 shows the physical principle of the permanent-magnet linear actuator under consideration. The actuator has a somewhat unusual system design. It consists of six permanent magnets with the magnetizing direction indicated by the arrows, four pairs of iron poles in form of flux concentrators for achieving high flux density in the air gap, four moving coils connected in series to the supply voltage (control input!) performing the Lorentz force generation and has a perpendicular geometry. In order to realize the required high acceleration against the disturbance force at the beginning of the valve opening, springs are also integrated into the exhaust valve actuators to support the motion. In general, for the valve opening and closing a moving distance of 8 mm must be covered within a time interval of about 4 ms.

0-7803-9098-9/05/$25.00 ©2005 AACC

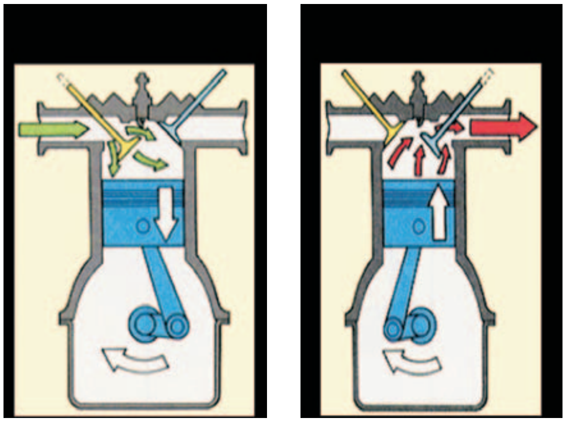

Fig. 1. On the left:Intake valve. On the right: Exhaust valve.

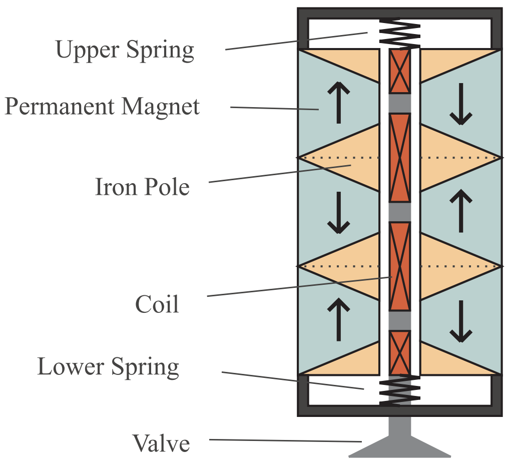

Fig. 2. Cross-section view of the perpendicular linear actuator.

The presented electromagnetic actuator can be modelled mathematically:

$$\dot{i}_{Coil} = -\frac{R_{Coil}}{L_{Coil}} i_{Coil} + \frac{u_{in} - lB_g(s, i_{Coil})v}{L_{Coil}} \quad (1)$$

$$\dot{s} = v \quad (2)$$

$$\dot{v} = \frac{lB_g(s, i_{Coil})}{m} i_{Coil} + \frac{-k_d v - k_f s + F_0}{m} \quad (3)$$

Equation (1) represents the electrical system of the actuator. Both equations (2) and (3) describe the mechanical behavior of the actuator as represented in Fig. 2, equation (3) also includes the magnetic system. The state representation is performed with the coil current i_{Coil}, the valve position (deviation) s and the actuator velocity v. In particular, the following expression

$$F_L = lB_g(s, i_{Coil}) i_{Coil}, \quad (4)$$

describes the Lorentz force generated by the actuator with the average air gap flux density $B_g(s, i_{Coil})$ and the effective coil length within the magnetic field l. In equation (1) $u_q = lB_g(s, i_{Coil})v$ represents the induced emf voltage. Furthermore m is the mass of the moving part of the actuator-valve system, F_0 the disturbance force (gas pressure) acting on the armature and F_{fric} the friction force modeled by

$$F_{fric} = k_d v, \quad (5)$$

with the damping coefficient k_d and

$$F_k = k_f s, \quad (6)$$

represents the spring force.

The parameter $B_g(s, i_{Coil})$ is strictly speaking a non-linear function of the state variables s and i_{Coil}. They are calculated from the source mmf of the permanent magnets and coils, the material and saturation depending magnetic reluctances and the relative position of the moving coils to the fixed iron poles against each other. Thus, the system description also becomes non-linear. On the other hand, however, due to the special system design using permanent magnets and flux concentrators, the operating point of the magnetic circuit is mainly determined by the magnet geometry and the demagnetization curve, see Fig. 3. The coil current only locally influences the field strength around the operating point (ΔH). An exact analytical expression between ΔH or $B_g(s, i_{Coil})$ and i_{Coil} is very difficult to derive as it is also depending on the saturation level of the iron parts and the leakage fluxes. However, a numerical solution can be obtained by applying finite-element-calculations point-by-point. Fig. 4 shows such a numerical calculation for the Lorentz force vs. coil current and valve position. Besides the weak dependence on the position s the electromagnetic force shows an almost linear relationship to the coil current which implies that the average air gap flux density is almost constant. Thus, in the investigations presented in this paper we assume a constant value of $B_g(s, i_{Coil})$.

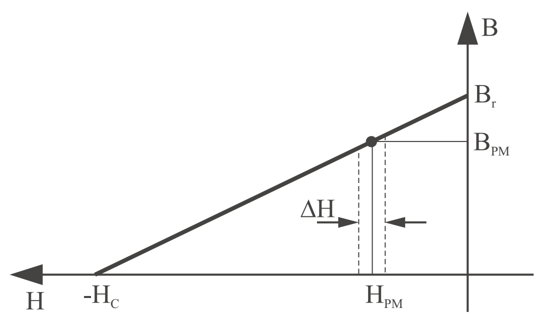

Fig. 3. Permanent-magnet demagnetization curve.

A. Some general issues

The goal of the actuator control is to ensure the valve opening and closing (operation cycle) based on some desired trajectories. During the opening process the gas pressure decreases relatively rapidly. The disturbance force for the actuator is mostly proportional to the gas pressure and its initial values at the beginning of the valve opening phase can vary between 0 and circa 400 N, depending on

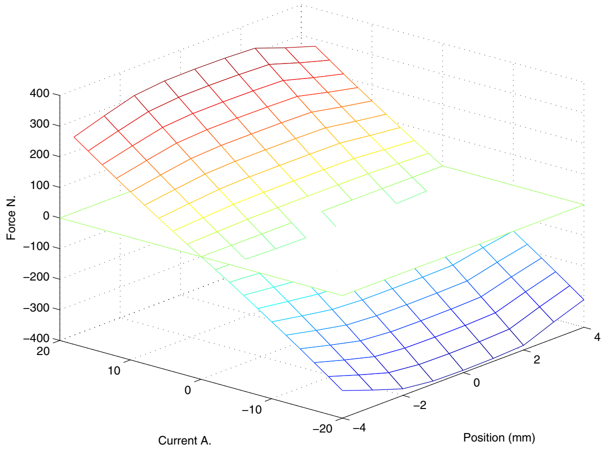

Fig. 4. Force vs. current and position, calculated using FEM.

the engine operating point and not predictable in advance. The cycle-to-cycle gas force deviation, though usually small in stationary operations, can be up to 200 N in extremly dynamic situations. In Fig 5 a tipical interpolated real measurement disturbance curves are depicted. Such a disturbance, in a first approximation, could be thought as an exponential signal with unknown time-varying initial condition and time constant. By modelling this disturbance as a zero-input response of a first order system with some unknown initial conditions, a possible approach is to try to identify the necessary time-varying parameters. The following discrete-time system can serve as the disturbance model

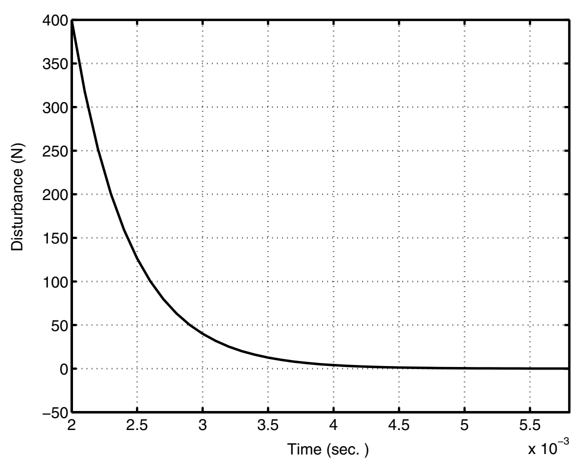

Fig. 5. Interpolation of the real pressure data.

$$d_{k+1} = a_k d_k, \tag{7}$$

with initial condition d_0 and a_k to be estimated. Kalman filter approach is now used to solve this coupled parameter and state estimation problem. Moreover, to avoid problems connected with extended and augmented Kalman estimator as described in [1] a particular combination of two new approaches is proposed.

The algorithm given below is based on discrete-time description of the system. Details on model discretization are omitted here for sake of brevity, except the note that the Heun's method was applied.

III. Robust and optimal Kalman estimator

The proposed algorithm is a combination of a robust Kalman filter as proposed in [5], an optimal Kalman filter as proposed in [7] and a least squares parameter estimation, unifying their advantages and also disadvantages.

Let us consider a system described by a four-map system (A, B, C, E), modelled by

$$\begin{aligned} x_{k+1} &= A_k x_k + B_k u_k + E_k d_k + \zeta_{1_k} \\ y_k &= C_k x_k + \zeta_{2_k}. \end{aligned}$$

where $x_k \in \mathcal{X}$ $(= \mathrm{R}^n)$, $u_k \in \mathcal{U}_k$ $(= \mathrm{R}^p)$, $d_k \in \mathcal{E}_k$ $(= \mathrm{R}^d)$, $y_k \in \mathcal{Y}_k$ $(= \mathrm{R}^q)$ denote respectively the state, the manipulable input, the disturbance and the informative output (measured output).

The following assumptions are made:

$\mathsf{rank}(E_k) = d$, $\mathsf{rank}(C_k) = q \geq d$ and $\mathsf{rank}(C_k E_k) = d$. The process noise ζ_{1_k} and the measurement noise ζ_{2_k} are zero-mean white noise sequences with the following covariances: $E(\zeta_{1_k}\zeta_{1_l}^T) = Q_k \delta_{k,l}$, $E(\zeta_{2_k}\zeta_{2_l}^T) = R_k \delta_{k,l}$, and $E(\zeta_{1_k}\zeta_{2_l}^T) = 0$, where $\delta_{k,l}$ denotes the Kronecker delta function. The following notation is used:

- $\bar{x}_{k/k}$ old state estimation, $\bar{x}_{k+1/k}$ and $\bar{x}_{k+1/k+1}$ a-priori and a-posteriori one-step state prediction.
- $\hat{x}_{k+1/k+1}$ a-posteriori estimation with disturbance correction.
- $\hat{d}_{k/k}$ old disturbances, $\hat{d}_{k+1/k}$ a-priori prediction, $\hat{d}_{k+1/k+1}$ a-posteriori estimation.
- $k^{\bar{x}}$, $k^{\hat{d}}$ Kalman gains for the state and the disturbance respectively.
- $P^{\bar{x}}$, $P^{\hat{d}}$ state's covariance matrix and disturbance's covariance matrix.

The main idea of development of the new hybrid Kalman filter is to organize the estimation procedure in two stages even though the two estimates are connected together. In Fig. 6 schematic representation of the algorithm is given. The algorithmic can be schematically represented as follows.

- An a-priori estimate of the state by using (10), as represented on the bottom-left block of Fig. 6.

- An a-priori estimation of the disturbance by using (14) as represented on the top-left block in Fig. 6.

- A a-posteriori estimate of the state by using (9), as represented on the bottom-right block of Fig. 6.

- An a-posteriori estimation of the disturbance by using (9) as represented on the top-right block in Fig. 6.

- A combination of a-posteriori state estimate and a-posteriori disturbance estimate as in relationship (8).

$$\begin{aligned}\hat{x}_{k+1/k+1} &= \bar{x}_{k+1/k+1} + V_{k+1}\hat{d}_{k+1/k+1} \\ P^{\hat{x}}_{k+1/k+1} &= P^{\bar{x}}_{k+1/k+1} + V_{k+1}P^{\bar{x}}_{k+1/k+1}V^{\mathrm{T}}_{k+1}\end{aligned} \tag{8}$$

$$\begin{aligned}\bar{x}_{k+1/k+1} &= \bar{x}_{k+1/k} + K^{\bar{x}}_{k+1}(y_{k+1} - C_{k+1}\bar{x}_{k+1/k}) \\ V_{k+1} &= E_{k+1} - K^{\bar{x}}_{k+1}C_{k+1}E_{k+1} \\ P^{\bar{x}}_{k+1/k+1} &= (I - K^{\bar{x}}_{k+1}C_{k+1})P^{\bar{x}}_{k+1/k}\end{aligned} \tag{9}$$

where

$$\bar{x}_{k+1/k} = A_k(\bar{x}_{k/k} + V_k\hat{d}_{k/k}) + B_k u_k \tag{10}$$
$$K^{\bar{x}}_{k+1} = P^{\bar{x}}_{k+1/k}C^{\mathrm{T}}_{k+1}G_{k+1} \tag{11}$$
$$P^{\bar{x}}_{k+1/k} = A_k P^{\bar{x}}_{k/k}A^{\mathrm{T}}_k + \bar{Q}_k \tag{12}$$
$$\bar{Q}_k = Q_k + A_k V_k P^{\hat{d}}_{k/k}V^{\mathrm{T}}_k A^{\mathrm{T}}_k \tag{13}$$
$$G_{k+1} = (C_{k+1}P^{\bar{x}}_{k+1/k}C^{\mathrm{T}}_{k+1} + R)^{-1}$$

$$\hat{d}_{k+1/k} = a_k\hat{d}_{k/k} \tag{14}$$

and its a-posteriori estimation is:

$$\begin{aligned}\hat{d}_{k+1/k+1} &= \hat{d}_{k+1/k} + \\ &K^{\hat{d}}_{k+1}(y_{k+1} - C_{k+1}\bar{x}_{k+1/k} - S_{k+1}\hat{d}_{k+1/k})\end{aligned} \tag{15}$$
$$S_k = C_k E_k$$

$$\begin{aligned}K^{\hat{d}}_{k+1} &= P^{\hat{d}}_{k+1/k}S^{\mathrm{T}}_{k+1}\times \\ &(C_{k+1}P^{\bar{x}}_{k+1/k}C^{\mathrm{T}}_{k+1} + R + S_{k+1}P^{\hat{d}}_{k+1/k}S^{\mathrm{T}}_{k+1})^{-1}\end{aligned}$$
$$P^{\hat{d}}_{k+1/k} = a_k P^{\hat{d}}_{k/k}a^{\mathrm{T}}_k + Q^{\hat{d}}_k$$
$$P^{\hat{d}}_{k+1/k+1} = P^{\hat{d}}_{k+1/k} - K^{\hat{d}}_{k+1}S_{k+1}P^{\hat{d}}_{k+1/k}.$$

In equation (14) a_k is calculated through the well known least squares method. If there is no a-priori knowledge about the disturbance, the start value is assumed to be equal to 1. Once a_k is available, the initial condition is estimated through disturbance model inversion and can be used for the next cycle. In particular, recall that $z = \exp(sT_s)$, where T_s is the sampling time interval, z is the position of the discrete pole and s the position of the continuous pole, the following equation is obtained:

$$a_t = -\frac{\log(a_k)}{T_s}$$

and the initial condition b_0 is calculated as

$$b_0 = \frac{\hat{d}_{k/k}}{\exp(-a_t * k * T_s)}.$$

Remark 1: The model assumed in (7) allows us to use the optimal structure of the algorithm and estimates the wanted disturbance within a few operation cycles even without any a-priori knowledge of the initial information, see Fig. (9). □

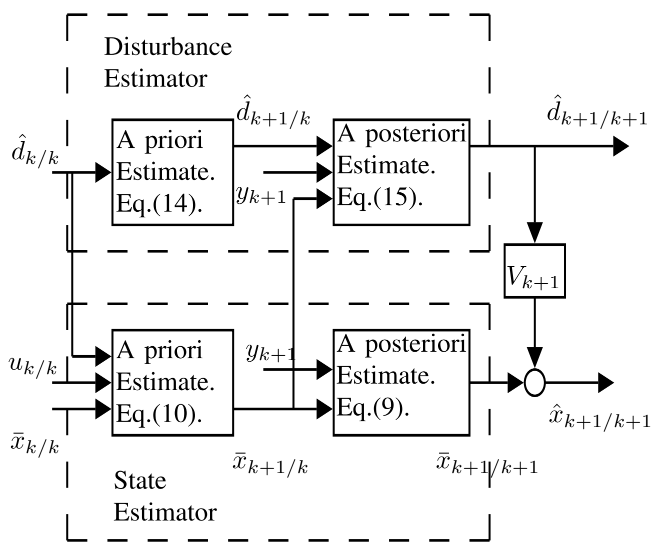

Fig. 6. Structure of the hybrid Kalman estimator.

A. Some comments and properties

The proposed Kalman filter combines the structure presented in [5] with the structure presented in [7]. In particular (12), (13) and (10) are parts of the robust algorithm in a *modified* optimal structure.

In other words, we use the knowledge of the disturbance as an input bias. In Fig. 6 the structure of the algorithm is depicted.

The algorithm has the following advantages and disadvantages:

Advantages

- Combining robust and optimal algorithm it is possible to estimate state and disturbance without using augmented Kalman filter to avoid the known problems as e.g. described in [1].

- The combination of the robust and optimal algorithm has lower calculation complexity compared with

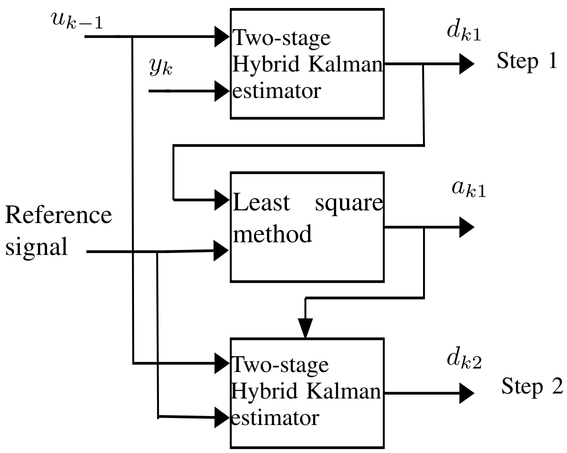

Fig. 7. Structure of the general twosteps hybrid Kalman estimator.

augmented algorithms.

- Good accuracy and robustness is achieved.

Disadvantages

- A model of the disturbance is needed for the algorithm.
- As stated in [7] a sufficient condition for the optimality of the estimation can not be given. Only one necessary condition is available : the modified bias filter covariance matrix $\bar{Q}_k$ must be positive semidefinite for all time.

IV. Simulation and results

Fig. 7 shows the general hybrid structure, which is an extension of the algorithm described above. The two-step structure can improve the estimation accuracy iteratively. By using the proposed two-step algorithm, as represented in Fig. 7, an improvement of the estimation is to remark. In Fig. 9 the estimation of a typical periodic disturbance is reported and it is also visible the approximation of the disturbance with one step and with two-steps. The amplitude initial condition is set to zero and it is shown that after some cycles the estimation is already good. Fig. 10 shows in detail the obtained benefit by using a two-step algorithm (with LSM determining a_k constant). An exact initial condition is assumed to be known and the test reveals the importance of the time constant estimation.

In many real applications, the model of the disturbance is not accurate, in these multi-step procedure can help. The information of the time constant is improved through least square method. In Fig. 11 results with two and three steps are summarized by using another typical pressure disturbance. It happens that in the first part of the disturbance estimation the Kalman filter has a reaction with a big Kalman-gain. This effect is due to the strong variation of time constat which is calculated during the steps. After that, the benefit is visible. Nevertheless, a multi-step algorithm

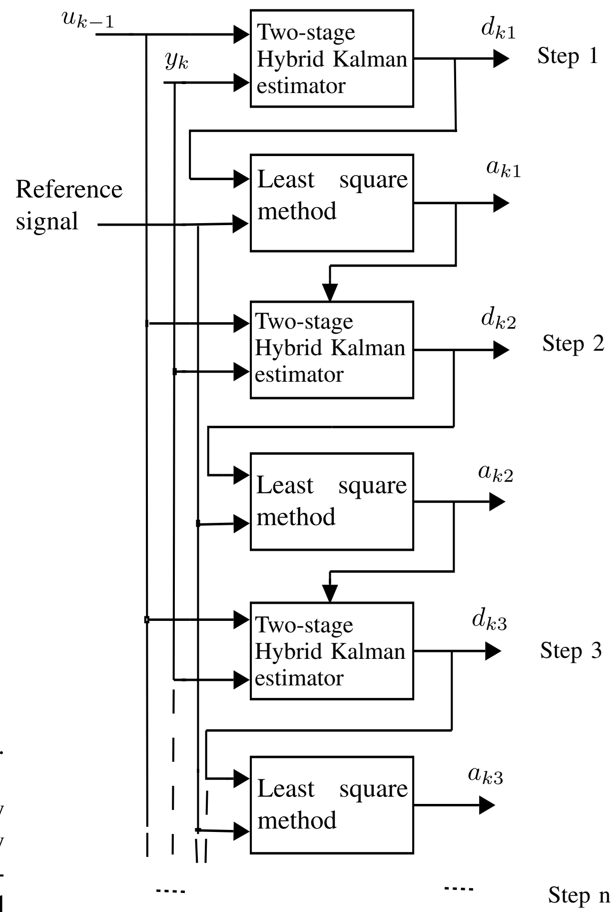

Fig. 8. Structure of the general multistep hybrid Kalman estimator.

presents some disadvantages, especially long calculation time and, as explained above, strong sensibility. In Fig. 12 and in Fig. 13 the estimation of position and velocity are respectively shown when a control structure based on MPC is performed as in [3]. From the presented simulation can remark the following points:

- when the structure and the initial condition of the disturbance is known, then one-step Kalman estimator produces good results.
- If just the structure of the disturbance is known, then good results are achieved in estimation of the disturbance by using a two-steps hybrid Kalman filter.
- If the structure of the disturbance is not known, then a multi-steps hybrid Kalman filter can be used in order to overcome the lack of knowledge.

V. Conclusions and Outlook

The paper deals with hybrid Kalman estimation integrating a robust and an optimal algorithm. A combination of two already known Kalman estimators is presented and a practical example with simulated physical data is shown.

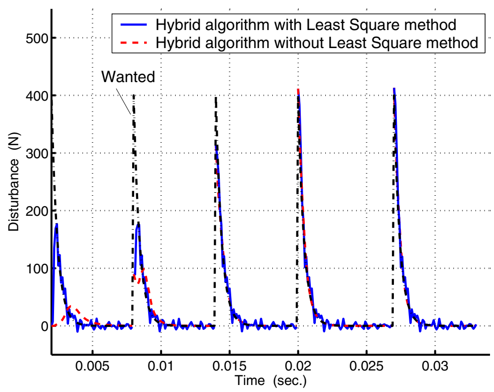

Fig. 9. Approximation of pressure disturbance. Hybrid two stage Kalman algorithm (one-step algorithm) (Solid line). Hybrid two stage Kalman algorithm (two-step algorithm) (Dashed line).

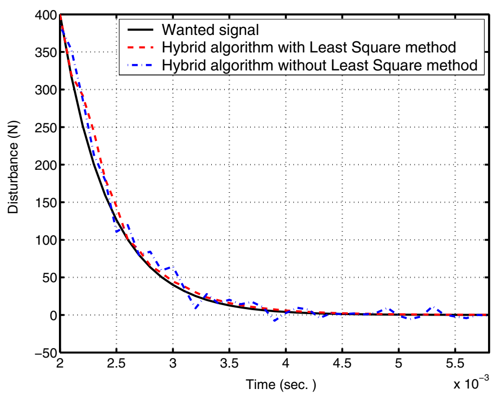

Fig. 10. Disturbance estimation. Dot line: One-step algorithm (without LSM). Dashed line: two-step algorithm (with LSM).

REFERENCES

[1] D. F. Bizup and D. E. Brown. The over-extended kalman filter- don't use. *Internal report number SIE-030001 in System and Information Dept. University of Virginia (USA)*, 2003.

[2] S. Butzmann, J. Melbert, and A. Koch. Sensorless control of electromagnetic actuators for variable valve train. In *Proc. SAE Technical Paper 2000-01-1225*, 2000.

[3] L. Chen, P. Mercorelli, and S. Liu. A two-stage kalman estimator for motion control using model predictive strategy. In *Proceedings of IEEE ICARCV*, 2004.

[4] W. Hoffmann and A. G. Stefanopoulou. Iterative learning control of electromechanical camless valve actuator. In *Proc. of American control conference*, 2001.

[5] C-S. Hsieh. Robust two-stage kalman filters for systems with unknown inputs. *IEEE Transactions on Automatic Control*, 45(12):2374–2378, 2000.

[6] C-S. Hsieh. General two-stage extended kalman filter. *IEEE Transactions on Automatic Control*, 48(2):289–293, 2003.

[7] C-S. Hsieh and F-C. Chen. Optimal solution of the two-stage kalman estimator. *IEEE Transactions on Automatic Control*, 44(1):194–199, 1999.

[8] K.S. Peterson and A. G. Stefanopoulou. Rendering the elecreomechanical valve actuator globally asymptotically stable. In *Proc. 42nd IEEE Conference on Decision and Control, Maui*, 2003.

[9] C. Tai and T. Tsao. Control of an electromechanical actuator for camless engines. In *Proceedings of the American control conference*, 2003.

[10] D. Haessig und B. Friedland. Separat-bias estimation with reduced-order kalman filters. *IEEE Transactions on Automatic Control*, 43(7):983–987, 1998.

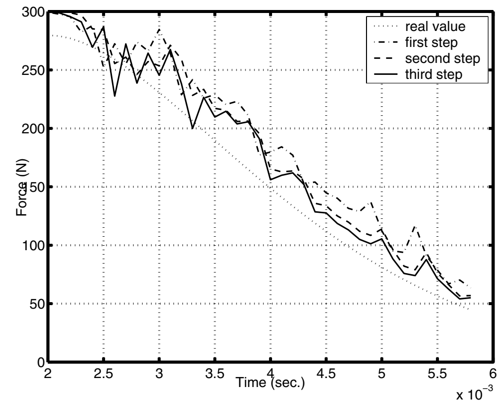

Fig. 11. Disturbance estimation. One-step algorithm (without LSM). Two-step and three-step algorithm (with LSM).

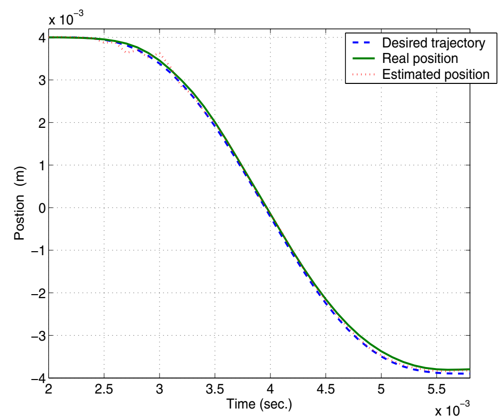

Fig. 12. Dashed line: desired position. Dot line: estimated position. Solid line: controlled position.

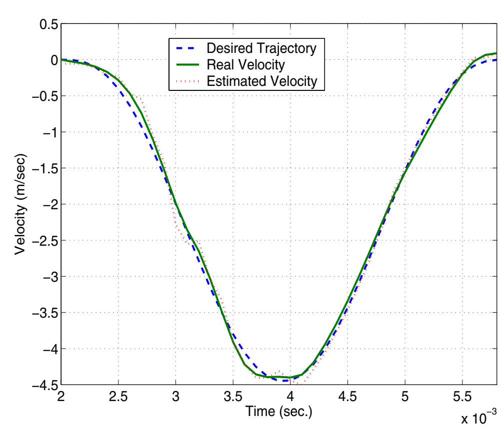

Fig. 13. Dashed line: desired velocity. Dot line: estimated velocity. Solid line: controlled velocity